Acta Cryst. (1977). B33, 743–754

The Crystal Structure and Superstructure of the *K* Phase, $Mn_{77}Fe_4Si_{19}$

BY CLARA BRINK SHOEMAKER AND DAVID P. SHOEMAKER

Department of Chemistry, Oregon State University, Corvallis, Oregon 97331, *USA*

(*Received* 6 *May* 1976; *accepted* 14 *August* 1976)

The *K* phase, $Mn_{77}Fe_4Si_{19}$, is monoclinic, $a = 13{\cdot}362$ (1), $b = 11{\cdot}645$ (1), $c = 8{\cdot}734$ (1) × 2 Å, $\beta = 90{\cdot}53$ (1)°, 110 × 2 atoms per unit cell, space group $C2$ (C_2^3). Reflections with odd l are quite weak, indicating that the full cell represents a superstructure. The structure model for the substructure was derived from the aspects of the diffraction pattern that resemble the σ-FeCr and the δ-MoNi patterns, and with the help of a three-dimensional Patterson function. It was refined by full-matrix anisotropic least squares with Mo $K\alpha$ diffractometer data to $R(F) = 0{\cdot}13$ (all 3244 reflections) or 0·06 (1932 reflections with $I > 2\sigma$). The substructure has rumpled layers and is entirely 'tetrahedrally close-packed' (tcp), with Mn(Fe) in the positions of coordination numbers (CN) 16, 15, and 14, and with mixtures of Mn(Fe) and Si in the positions of CN 12. Since the substructure did not show evidence of 'elongated atoms' (marked apparent thermal anisotropies) the superstructure was assumed to be substitutional in regard to occupancy of CN 12 sites by Mn(Fe) or Si. The superstructure was solved with the aid of a Patterson function calculated with superstructure data only, and with least-squares refinement of site occupancies for the CN 12 atoms. Different CN 12 sites were found to be occupied by Mn(Fe) atoms, Si atoms, or mixtures of Mn(Fe) and Si. The alteration between the two subcells is such as to allow Si atoms to be everywhere coordinated only by Mn(Fe). In this the *K* phase resembles the ν phase, $Mn_{82}Si_{18}$, and the *X* phase, $MN_{45}Co_{40}Si_{15}$, with plane-layered tcp structures, but differs from the *D* phase, Mn_5Si_2, with a somewhat 'non-ideal' tcp structure in which there are a few Si–Si contacts.

Introduction

The *K* phase was discovered by K. P. Gupta (1964). It is found at 1000 °C in the Mn–Si–Fe system at about 18 at.% Si and with Fe content varying between 1 and 6 at.% Fe. A sample was kindly made available to us by Professor Paul A. Beck, University of Illinois. We undertook to determine its crystal structure as part of a program to investigate the role of Si as a component in the family of transition-metal alloy structures described as 'tetrahedrally close-packed' (tcp) (Shoemaker & Shoemaker, 1971*b*). These are structures in which the interstices are exclusively tetrahedral and in which, ideally, the atomic sites have coordination numbers (CN) 12, 14, 15, and 16 only (Frank & Kasper, 1959). Previous work on the ν phase, $Mn_{82}Si_{18}$, and the *X* phase, $Mn_{45}Co_{40}Si_{15}$, showed them to be plane-layered tcp structures in which Si atoms were coordinated exclusively by Mn (Shoemaker & Shoemaker, 1971*a*; Manor, Shoemaker & Shoemaker, 1972). At about the same time that the initial *K* phase work was undertaken a decade ago, we also undertook to determine the structure of the *D* phase, $V_{26{\cdot}5}Fe_{44}Si_{29{\cdot}5}$. This structure was eventually refined with data obtained for the isotypic Mn_5Si_2 (Shoemaker & Shoemaker, 1976), and proved to be predominately tcp but with some 'non-ideal' features, namely the existence of 4-coordinated bonds [*i.e.* bonds to ligands of polyhedron surface coordination number (SCN) four] and of sites of CN 13 and 11 as well as CN 12, 14, and 16. In that structure there are a few Si–Si contacts ('bonds'). The results of early work on the *K* phase revealed the correct atomic arrangement but could not identify sites occupied predominantly by Si, and accordingly could not indicate whether there are or are not Si–Si contacts. In large part this resulted from the existence in the *K* phase of a superstructure which might be (and is now shown to be) substitutional. The full determination of the structure, including the superstructure, as described in this paper, shows that Si–Si contacts are probably absent, causing the structure to resemble in this respect the ν phase and the *X* phase and not the *D* phase. Some uncertainty remains because some neighboring sites in the superstructure are occupied by mixtures, and the correlation of their occupancies is beyond the power of our diffraction data to determine. (This is also true in the ν and *X* phases examined.)

Experimental

Intensity data for a crystal fragment in arbitrary orientation were collected with Mo $K\alpha$ radiation on an automated Syntex $P\bar{1}$ diffractometer equipped with a graphite monochromator. A θ–2θ scan was used; the scan speed was 1 deg min^{-1}, the 2θ range was 2·0° plus the $\alpha_1\alpha_2$ angular separation. Background readings were made at the beginning and the end of each scan range; the ratio of background time to scan time was 1 to 2. All reflections in a half sphere of reciprocal space

were measured out to $2\theta = 30°$, in a quarter sphere out to $2\theta = 70°$. Superstructure reflections were only measured out to $2\theta = 45°$. The dimensions of the crystal varied between 0·065 and 0·075 mm, and an absorption correction was applied for a spherical crystal with $\mu r = 0{\cdot}74$, corresponding to absorption factors ranging from 2·75 to 2·60. In a later stage of the refinement a secondary extinction correction factor was applied in the form: $F_o^{corr} = F_o(1 + gI_o)$ (Zachariasen, 1963). The value of g was refined with the least-squares program *NUCLS* (see below); the largest correction was 4%. The real part of the anomalous dispersion correction was taken into account (Cromer & Liberman, 1970).

Structure model for the subcell

The crystal data for the K phase are compared with those for the σ phase (Bergman & Shoemaker, 1954) and the δ phase (Shoemaker & Shoemaker, 1963) in Table 1. The δ phase is pseudo-tetragonal and its cell dimensions are similar to those of the σ phase, except for an approximate doubling of the c axis. It contains puckered σ-phase-type layers (consisting of hexagons and triangles, with the hexagons in successive layers antisymmetrically superimposed) perpendicular to the a and the b axes. The K phase diffraction pattern is very similar to that of the δ phase, but the σ-phase-type 'nets' are the hhl and the $h\bar{h}l$ planes through the origin of the reciprocal lattice, and these planes enclose an angle of about 98°, rather than 90° as in the δ phase. The resulting structure is monoclinic and the diffraction symmetry is $2/m$. The systematic absences are: hkl with $h + k$ even; these permit space groups $C2/m$, $C2$, and Cm. The three-dimensional Patterson function did not support a mirror plane perpendicular to the b axis and the space group was therefore assumed to be $C2$.

Table 1. *Crystal data for the K phase (compared with those for the σ phase and the δ phase)*

	K $Mn_{77}Fe_4Si_{19}$	σ $Cr_{46}Fe_{54}$	δ MoNi
F.W./100	49·872		
a(Å)	13·362 (1)	8·800	9·108
b	11·645 (1)		9·108
c	8·734 (1) × 2	4·544	8·852
β(°)	90·53 (1)		
V(Å^3)	1359·01 × 2	391·9	734·3
λ(Mo $K\alpha$) (Å)	0·710688		
Space group	$C2$ (C_2^3)	$P4_2/mnm$	$P2_12_12_1$
Atoms/cell	110 × 2	30	56
D_m (g cm^{-3})	6·46 (10)		
D_x	6·70		
F(000)	2524 × 2		
μ(Mo $K\alpha$) (cm^{-1})	212·6		
'σ net'	hhl, $h\bar{h}l$	$hk0$	$h0l$, $0kl$

The halved diagonals of the (001) plane correspond to the a and the b axes of the δ phase, and the primitive K-phase cell corresponds roughly to the δ-phase cell in volume and number of atoms.

A structure model for the subcell of the K phase was derived by trial shifting σ-phase-type layers parallel to the $(1\bar{1}0)$ plane in such a way that a high peak in the three-dimensional Patterson function was explained. These layers were then puckered so that good coordination for some of the atoms resulted. The twofold axis appeared to be in the position of a pseudo-twofold axis in the δ phase. This model, derived several years ago at Massachusetts Institute of Technology, contained many atoms with irregular coordinations and could not be refined with the very inadequate data set obtained with Cu $K\alpha$ radiation. With the new data set obtained as described above with Mo $K\alpha$ radiation of a smaller and more nearly spherical crystal the initial model could be refined to a structure in which all atoms had 'regular' tcp coordinations.

Structure refinement

Data treatment

The data reduction and initial structure factor calculations were done on the Oregon State University CDC 3300 computer with local versions of the programs *STUDIT, INCOR* (Zalkin), and *LSLONG* (based on Zalkin's modification of the Gantzel–Sparks–Trueblood refinement program). The scattering factors for the neutral atoms were taken from *International Tables for X-ray Crystallography* (1962) and corrected for the real part of the anomalous dispersion (Cromer & Liberman, 1970) with $f' = 0{\cdot}295$ for Mn and 0·072 for Si. The intensities of hkl and $h\bar{k}l$ were averaged when both were measured ($2\theta < 30°$) and the weights were based on the standard errors in the intensities I_o as estimated with the equation $\sigma(I_o) = [C + Bt^2 + (0{\cdot}02C)^2 + (0{\cdot}02Bt)^2]^{1/2}$ (C is the integrated count, B is the total background count, $t = 2$ is the ratio of the scan time over the background time). All reflections were used in the refinements; the reflections with intensities lower than the background were entered with 0 or a very small positive value. The refinements were done on the Lawrence Berkeley Laboratory CDC 7600 computer from a remote terminal with the *LESQ* and the *NUCLS* programs contained in Zalkin's XRAY76 program system.

The average structure of the subcell

Since the superstructure reflections indicating a doubling of the c axis are very weak (the largest superstructure intensity is about 2% of the largest substructure intensity) and few in number (of the 997

measured out to $2\theta = 45°$ only 160 are $>2\sigma$ and only 81 are $>3\sigma$) the structure of the average subcell was determined first. Preliminary least-squares refinement of the model with a limited data set ($2\theta < 45°$) showed that all 29 atoms in the asymmetric unit (26 in general positions and 3 on twofold axes) had the normal coordinations of the tcp structures (Shoemaker & Shoemaker, 1969), namely CN 16, 15, 14 and 12, and that a limited range of isotropic thermal parameters resulted when the atoms with CN 16 and 15 were given the Mn scattering factor and the atoms with CN 14 and 12 the scattering factor of a mixture of 58 at.% Mn and 42 at.% Si. [Because of the small amount of Fe present and the close similarity between Fe and Mn scattering factors, the distinction between Fe and Mn is frequently ignored throughout this paper; both are represented

Table 2. *Agreement indices for the least-squares refinements of the K phase*

	Number of reflections	Thermal parameters	Number of variables	$R(F)$	$R_w(F)$	S*
Subcell	3244	Isotropic	134	0·138	0·028	1·081
	3244	Anisotropic	265	0·132	0·025	0·961
	1932 $I>2\sigma$ only	Anisotropic	265	0·062	0·022	1·140
Supercell	4241	Isotropic	92	0·170	0·031	1·002
	2090 $I>2\sigma$ only			0·073	0·035	1·700
Superstructure reflections only† ($2\theta < 45°$)	997	Isotropic		0·556		1·03
	160 $I>2\sigma$			0·211	0·196	2·73
	81 $I>3\sigma$			0·155	0·158	

* $S = [\Sigma\, w(F_c - F_o)^2/(n_{\text{refl.}} - n_{\text{var.}})]^{1/2}$.

† The values given for S were after refinement of superstructure occupancies only; those given for R and R_w were after additional positional refinement.

Table 3. *Atomic parameters for the average subcell of the K phase*

All atoms are in positions 4(*c*), except atoms 18 and 19 in 2(*a*), and atom 17 in 2(*b*). The root-mean-square displacements (RMSD) are given in Å along the principal axes of the vibrational ellipsoids. Here and in subsequent tables Mn is used to designate Mn(Fe), and MS is used to designate mixtures of Mn(Fe) with Si.

CN		x	y	z	RMSD 1	RMSD 2	RMSD 3	m	f_o	at. % Mn
16	Mn(1)	0·08276 (25)	0·21539	0·09210 (36)	0·072	0·095	0·117	2·00	25·0	100·0
16	Mn(12)	0·10278 (29)	−0·01260 (40)	0·54695 (38)	0·073	0·105	0·146	2·00	25·0	100·0
16	Mn(17)	½	0·08763 (51)	½	0·056	0·108	0·134	1·00	25·0	100·0
16	Mn(27)	0·27912 (24)	0·37596 (42)	0·67427 (42)	0·072	0·088	0·137	2·00	25·0	100·0
15	Mn(16)	0·43790 (27)	−0·04462 (44)	0·72980 (39)	0·071	0·102	0·112	2·00	25·0	100·0
15	Mn(21)	0·40253 (27)	0·31837 (43)	0·91570 (39)	0·073	0·080	0·125	2·00	25·0	100·0
14	Mn(2)	0·03079 (24)	0·20547 (44)	0·37435 (37)	0·075	0·092	0·127	2·00	25·0	100·0
14	Mn(4)	0·18052 (24)	0·19317 (42)	0·58915 (37)	0·055	0·079	0·093	2·00	25·0	100·0
14	MS(5)	0·47458 (26)	0·16857 (44)	0·16412 (44)	0·069	0·113	0·141	1·99 (3)	24·9	99·0
14	Mn(11)	0·18922 (26)	0·02974 (44)	0·05239 (39)	0·079	0·106	0·113	2·00	25·0	100·0
14	Mn(13)	0·36205 (25)	0·01691 (46)	0·23239 (39)	0·068	0·100	0·116	2·00	25·0	100·0
14	MS(19)	½	−0·06048 (57)	0	0·081	0·104	0·125	0·96 (2)	23·9	90·0
14	Mn(24)	0·35691 (25)	0·22873 (45)	0·41435 (37)	0·072	0·094	0·109	2·00	25·0	100·0
14	Mn(26)	0·20874 (27)	0·33122 (43)	0·34124 (39)	0·075	0·105	0·124	2·00	25·0	100·0
14	Mn(28)	0·39339 (26)	0·38221 (45)	0·18598 (37)	0·076	0·091	0·107	2·00	25·0	100·0
14	MS(29)	0·19869 (27)	0·38468 (46)	0·02986 (40)	0·056	0·096	0·126	1·89 (3)	23·6	88·0
12	MS(3)	0·28949 (29)	0·21349 (55)	0·13342 (44)	0·061	0·077	0·084	1·86 (3)	19·0	45·0
12	MS(6)	0·36310 (31)	0·16908 (47)	0·69219 (44)	0·069	0·095	0·114	2·19 (4)	22·3	75·0
12	MS(7)	0·19674 (28)	0·11035 (50)	0·32278 (46)	non-positive definite			1·92 (3)	19·5	50·0
12	MS(8)	0·08445 (31)	0·10696 (48)	0·81286 (46)	0·067	0·085	0·104	2·17 (3)	22·1	73·5
12	MS(9)	0·37139 (31)	0·08633 (51)	0·95125 (45)	0·070	0·100	0·128	2·11 (4)	21·5	68·0
12	MS(10)	0·05701 (33)	−0·00025 (51)	0·25945 (49)	0·087	0·122	0·139	2·05 (4)	20·9	62·5
12	MS(14)	0·30651 (32)	0·02724 (49)	0·51169 (47)	0·064	0·092	0·111	1·95 (3)	19·9	53·5
12	MS(15)	0·24369 (28)	0·01874 (47)	0·76504 (43)	0·063	0·082	0·111	2·07 (4)	21·1	64·0
12	MS(18)	0	0·00110 (66)	0	0·078	0·132	0·136	1·15 (3)	23·4	85·5
12	MS(20)	0·08413 (31)	0·37692 (53)	0·55264 (46)	0·050	0·090	0·101	1·88 (3)	19·2	46·5
12	MS(22)	0·52655 (29)	0·31520 (48)	0·37206 (46)	0·084	0·096	0·123	2·08 (4)	21·2	65·0
12	MS(23)	0·23168 (25)	0·21331 (48)	0·87748 (36)	0·045	0·059	0·100	2·23 (3)	22·7	79·0
12	MS(25)	0·08455 (36)	0·31476 (54)	0·81122 (53)	0·049	0·103	0·119	1·83 (4)	18·6	41·5

by Mn(Fe) or by Mn for short.] Two refinement cycles were then run with program *NUCLS* (see above) including all 3244 reflections and 134 variable parameters, namely the scale factor, extinction parameter, 29 isotropic thermal parameters, 80 positional parameters [the y parameter of atom Mn(1) was not allowed to vary] and the occupancy parameters for the 23 atoms with CN 12 or CN 14. The agreement indices

Table 4. *Interatomic distances in the average subcell of the K phase*

The standard deviations are estimated to range between 0·004 and 0·008 Å. Distances occurring twice when reading down are underlined. Asterisks indicate major bonds.

Atom	CN	Mn(1) 16	Mn(12) 16	Mn(17) 16	Mn(27) 16	Mn(16) 15	Mn(21) 15	Mn(2) 14	Mn(4) 14	MS(5) 14	Mn(11) 14	Mn(13) 14	MS(19) 14	Mn(24) 14	Mn(26) 14	Mn(28) 14	MS(29) 14	
Mn(1)	16	2.723*				3.212		2.570*			2.613*		2.944		3.055		2.568*	Mn(1)
Mn(12)	16		2.859*		2.822*			3.102	2.636*					3.078	3.249	2.635*		Mn(12)
								3.183										
Mn(17)	16					2.668*				3.097		3.076		2.625*				Mn(17)
Mn(27)	16		2.822*				2.748*		2.608*		3.011	2.635*		3.036	3.093		3.297	Mn(27)
Mn(16)	15	3.212		2.668*				3.079		2.893		2.784	2.501*		2.508*		2.915	Mn(16)
Mn(21)	15				2.748*		2.980			2.499*	2.765					2.479*	3.010	Mn(21)
										2.939						2.970		
Mn(2)	14	2.570*	3.102			3.079		2.351*	2.734						2.810			Mn(2)
			3.183						2.848									
Mn(4)	14		2.636*		2.608*			2.734						2.850	2.726			Mn(4)
								2.848										
MS(5)	14			3.097		2.893	2.499*			2.952		2.398*	3.049	2.793		2.721		MS(5)
							2.939											
Mn(11)	14	2.613*			3.011		2.765					2.786				2.909	2.373*	Mn(11)
Mn(13)	14			3.076	2.635*	2.784				2.598*	2.786		2.898	2.935			2.871	Mn(13)
MS(19)	14	2.944				2.501*				3.049		2.898					2.741	MS(19)
Mn(24)	14		3.078	2.625*	3.036				2.850	2.793		2.935			2.393*	2.725		Mn(24)
Mn(26)	14	3.053	3.249		3.093	2.508*		2.810	2.726					2.393*		2.888	2.792	Mn(26)
Mn(28)	14		2.635*				2.479*			2.721	2.909			2.725	2.888		2.929	Mn(28)
							2.970											
MS(29)	14	2.568*			3.297	2.913	3.010				2.373*	2.871	2.741		2.792	2.926		MS(29)
MS(3)	12	2.783					2.728			2.540	2.619	2.629		2.612	2.525	2.447	2.499	MS(3)
MS(6)	12			2.668	2.662	2.701	2.663		2.608	2.496				2.525				MS(6)
MS(7)	12	2.796	2.740		2.749			2.525	2.530		2.542	2.592		2.662	2.582			MS(7)
MS(8)	12	2.704	2.721					2.515	2.553		2.663					2.634		MS(8)
		2.747																
MS(9)	12					2.624	2.752			2.491	2.679	2.589	2.458				2.534	MS(9)
										2.496								
MS(10)	12	2.927	2.583		2.680		2.666	2.622			2.564					2.653		MS(10)
			2.740															
MS(14)	12		2.781	2.682	2.649	2.711			2.655			2.559		2.587	2.628			MS(14)
MS(15)	12		2.691			2.718			2.679		2.623				2.459	2.466	2.493	MS(15)
MS(18)	12	2.843					2.598				2.587					2.574		MS(18)
MS(20)	12			2.736	2.805	2.644		2.602	2.516			2.584			2.554			MS(20)
						2.665		2.626										
MS(22)	12		2.713	2.899	2.725		2.694			2.583				2.511		2.522		MS(22)
			2.744											2.620				
MS(23)	12	2.746			2.676		2.609		2.614		2.691						2.441	MS(23)
MS(25)	12	2.662			2.959	2.646		2.564	2.731			2.490	2.478				2.565	MS(25)
		2.713																
		Mn(1)	Mn(12)	Mn(17)	Mn(27)	Mn(16)	Mn(21)	Mn(2)	Mn(4)	MS(5)	Mn(11)	Mn(13)	MS(19)	Mn(24)	Mn(26)	Mn(28)	MS(29)	

Atom	CN	MS(3) 12	MS(6) 12	MS(7) 12	MS(8) 12	MS(9) 12	MS(10) 12	MS(14) 12	MS(15) 12	MS(18) 12	MS(20) 12	MS(22) 12	MS(23) 12	MS(25) 12	
Mn(1)	16	2.783		2.796	2.704		2.927			2.843			2.746	2.662	Mn(1)
					2.747									2.713	
Mn(12)	16			2.740	2.721		2.583	2.781	2.691			2.713			Mn(12)
							2.740					2.744			
Mn(17)	16		2.668					2.682			2.736	2.899			Mn(17)
Mn(27)	16		2.662	2.749			2.680	2.649			2.805	2.725	2.676	2.959	Mn(27)
Mn(16)	15		2.701			2.624		2.711	2.718		2.644			2.646	Mn(16)
											2.665				
Mn(21)	15	2.728	2.663			2.752	2.666			2.598		2.694	2.609		Mn(21)
Mn(2)	14			2.523	2.513		2.622				2.602			2.564	Mn(2)
											2.626				
Mn(4)	14		2.608	2.530	2.553			2.655	2.679		2.516		2.614	2.731	Mn(4)
MS(5)	14	2.540	2.496			2.491						2.583			MS(5)
						2.496									
Mn(11)	14	2.619		2.542	2.663	2.679	2.564		2.623	2.587			2.691		Mn(11)
Mn(13)	14	2.629		2.592		2.589		2.559			2.584			2.490	Mn(13)
MS(19)	14					2.458								2.478	MS(19)
Mn(24)	14	2.612	2.525	2.662				2.587				2.511			Mn(24)
												2.620			
Mn(26)	14	2.525		2.582				2.628	2.459		2.554				Mn(26)
Mn(28)	14	2.447			2.634		2.653		2.466	2.574		2.522			Mn(28)
MS(29)	14	2.499				2.534			2.493				2.441	2.565	MS(29)
MS(3)	12			2.398		2.440							2.358		MS(3)
MS(6)	12					2.461		2.401	2.457			2.324	2.454		MS(6)
MS(7)	12	2.398					2.331	2.401							MS(7)
MS(8)	12						2.347		2.403	2.345			2.388	2.420	MS(8)
MS(9)	12	2.440	2.461						2.475				2.463		MS(9)
MS(10)	12			2.331	2.347					2.384		2.400			MS(10)
MS(14)	12		2.401	2.401					2.376		2.352				MS(14)
MS(15)	12		2.457		2.403	2.475		2.376					2.475		MS(15)
MS(18)	12				2.345		2.384								MS(18)
MS(20)	12							2.352			2.421			2.372	MS(20)
MS(22)	12		2.324				2.400					2.351			MS(22)
MS(23)	12	2.358	2.454		2.388	2.463			2.475					2.361	MS(23)
MS(25)	12				2.420						2.372		2.361		MS(25)
		MS(3)	MS(6)	MS(7)	MS(8)	MS(9)	MS(10)	MS(14)	MS(15)	MS(18)	MS(20)	MS(22)	MS(23)	MS(25)	

at the end of this isotropic refinement are given in the first line of Table 2. All CN 14 sites appeared to be occupied by Mn atoms, except three sites that might contain small percentages of Si. All CN 12 sites were occupied by various mixtures of Mn and Si. Two cycles with all reflections and 265 variable parameters (extinction, 168 anisotropic thermal parameters, 80 positional parameters, and 16 occupancy factors for the 13 sites with CN 12 and three sites with CN 14) led to the agreement indices given on the second line of Table 2. Three anisotropic cycles in which reflections with $I < 2\sigma$ were given zero weight resulted in the final parameters given in Table 3 and agreement indices given on the third line of Table 2. The differences in positional parameters obtained in the two types of anisotropic refinement were much smaller than σ. The interatomic distances given in Table 4 are based on the positional parameters given in Table 3. Atom MS(7), which had a small isotropic thermal parameter ($0{\cdot}30 \pm 6$ Å^2), gave a non-positive-definite result in the anisotropic refinement. [MS signifies a mixture of Mn(Fe) and Si.]

The superstructure

The root-mean-square displacements of the atoms obtained in the anisotropic refinement are of the order of $0{\cdot}1$ Å in all directions, which indicates that there are no large differences in the positional parameters between corresponding sites in the two subcells of the supercell. We therefore assumed that corresponding sites in the two subcells differ only in occupancy in the first approximation, and that the sites that differ in occupancy are those that were found to be occupied by a mixture of Mn(Fe) and Si in the average structure.

The space group of the supercell is also $C2$, but half of the twofold rotation axes and twofold screw axes of the average structure are replaced by corresponding elements of pseudosymmetry ('color symmetry'), relating sites of approximately the same position, but different occupancy. These are the symmetry elements with the open lenses in Fig. 1. In the average structure atoms 18 (CN 12) and 19 (CN 14) lie on one set of twofold axes, and atom 17 (CN 16) lies on the second set. It seemed likely that the first set of axes would be retained in the supercell since then atoms 18 and 19 could have different occupancies in the two subcells. Collaborative evidence of this was provided by the $h0l$ layer of a Patterson function calculated with the superstructure reflections only: interactions between pairs of atoms that were found to be occupied by mixtures of about 50% Mn in the average structure (atoms 3, 7, 14, 20, 25) across the first set of axes were generally in positive areas, across the second set of axes in negative areas. Preliminary least-squares refinements were carried out on the superstructure structure factors only. In each such refinement the occupancy of one atom of each pair of CN 12 atoms ('unprimed' in one subcell and 'primed' in the other) was varied, except that the occupancies of one pair (initially 3 and 3′ or 25 and 25′, later other pairs) were kept constant at total segregation. These refinements consistently gave the same qualitative pattern of relative enrichment and depletion of Mn on corresponding sites in the two subcells. The starting model for the superstructure thus obtained contained chains of sites with alternate enrichment and depletion of Mn. Fig. 1 shows part of the superstructure model; the alternation, however, is not everywhere clear from the figure since several atoms (see Fig. 1 caption) are at elevations significantly above those indicated, and symmetry-related atoms in neighboring layers are not shown although some of them are involved in the alternation. This model was refined by the following procedure.

The scattering factor (without temperature factor) for a particular CN 12 atom (j) can be written

$$f_j = \bar{f}_j + y_j \Delta f,\ f_j' = \bar{f}_j - y_j \Delta f$$

where

$$\bar{f}_j \equiv \tfrac{1}{2}(f_j + f_j') = a_j f_{\mathrm{Mn}} + (1 - a_j) f_{\mathrm{Si}} = f_{\mathrm{Si}} + a_j \Delta f$$

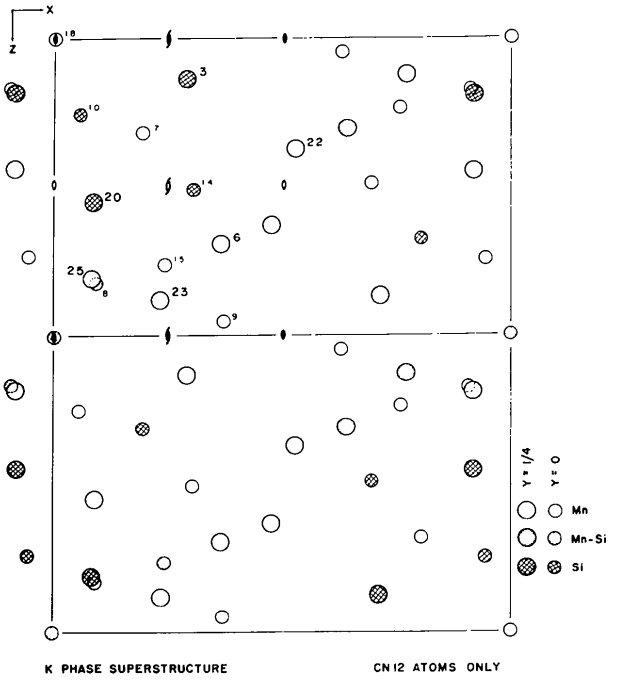

Fig. 1. Arrangement of the CN 12 atoms in the layers at $y \simeq 0$ and $\frac{1}{4}$ in the superstructure of the K phase. Every kind of CN 12 atom is shown once in each subcell of the figure. Atoms 7, 8, 9, 20, 22, and 25 are at elevations significantly above those indicated by the symbols. The symmetry elements with the closed lenses shown in the upper half of the cell apply alike to the substructure and the superstructure, those with the open lenses apply to the average substructure only and are elements of pseudosymmetry for the superstructure.

and

$$\Delta f \equiv f_{Mn} - f_{Si} .$$

The $\bar{f}_j$ are the scattering factors obtained from the average substructure refinement. The values of a_j were determined from two refinement cycles with the substructure data in which the isotropic thermal parameters were also varied but the scale factor and positional parameters were fixed. Nine cycles of least-squares refinement were then carried out with the superstructure data in which every CN 12 atom, and the three CN 14 atoms with $\bar{f}_j$ smaller than f_{Mn} (see Table 3), were entered with scattering factor Δf. The parameters y_j were refined in the same manner as occupancy parameters; the scale factor and the thermal and positional parameters were fixed and all measured superstructure reflections were used. The contents of

Table 5. *Atomic parameters for the supercell of the K phase*

CN		*x,x'*	*y,y'*	*z,z'**	*B*(Å²)	$a_j \pm y_j$	%Mn adj.	*m*†
16	Mn(1)	0·0827 (2)	0·2154	0·0458 (2)	0·82 (4)			
16	Mn(12)	0·1032 (2)	−0·0127 (3)	0·2733 (2)	1·00 (4)			
16	Mn(17)	0·4988 (7)	0·0878 (3)	0·2471 (5)	0·93 (6)		100·	
16	Mn(27)	0·2792 (2)	0·3758 (4)	0·3371 (2)	0·87 (4)			
15	Mn(16)	0·4379 (2)	−0·0443 (4)	0·3648 (2)	0·70 (4)			
15	Mn(21)	0·4027 (2)	0·3183 (4)	0·4579 (2)	0·70 (4)			
14	Mn(2)	0·0309 (2)	0·2053 (4)	0·1871 (2)	0·78 (4)			
14	Mn(4)	0·1807 (2)	0·1929 (3)	0·2944 (2)	0·59 (4)			
14	Mn(5)	0·4760 (5)	0·1672 (6)	0·0788 (4)	0·92 (6)	1·10 (6)	100·	
	MS(5′)	0·4733 (6)	0·1707 (7)	0·5856 (4)		0·77	87·	1·16
14	Mn(11)	0·1889 (2)	0·0297 (4)	0·0259 (2)	0·74 (4)			
14	Mn(13)	0·3619 (2)	0·0170 (4)	0·1162 (2)	0·73 (4)			
14	MS(19)	½	−0·0560 (10)	0	0·81 (9)	0·80 (8)	77·	1·10
	Mn(19′)	½	−0·0642 (9)	½		0·97	100·	
14	Mn(24)	0·3570 (2)	0·2286 (4)	0·2073 (2)	0·69 (4)			
14	Mn(26)	0·2087 (2)	0·3311 (4)	0·1708 (2)	0·92 (4)			
14	Mn(28)	0·3932 (2)	0·3825 (4)	0·0930 (2)	0·72 (4)			
14	Mn(29)	0·2014 (5)	0·3841 (7)	0·0132 (4)	0·82 (6)	1·03 (6)	100·	
	MS(29′)	0·1950 (6)	0·3853 (8)	0·5172 (4)		0·70	73·	1·08
12	Si(3)	0·2847 (9)	0·2124 (12)	0·0674 (8)	0·49 (7)	−0·01 (5)	0·	
	Mn(3′)	0·2924 (5)	0·2124 (6)	0·5666 (4)		0·96	100·	
12	Mn(6)	0·3639 (5)	0·1696 (7)	0·3449 (4)	0·64 (8)	0·96 (6)	100·	
	MS(6′)	0·3625 (8)	0·1682 (9)	0·8480 (6)		0·49	45·	0·92
12	Mn(7)	0·1951 (5)	0·1121 (6)	0·1619 (4)	0·30 (6)	1·12 (6)	100·	
	Si(7′)	0·2003 (9)	0·1051 (12)	0·6604 (7)		−0·08	0·	
12	MS(8)	0·0828 (8)	0·1086 (9)	0·4062 (6)	0·54 (6)	0·49 (5)	38·	0·90
	Mn(8′)	0·0854 (6)	0·1048 (7)	0·9064 (4)		0·89	100·	
12	MS(9)	0·3767 (7)	0·0838 (9)	0·4755 (6)	0·78 (8)	0·26 (6)	36·	0·88
	Mn(9′)	0·3671 (5)	0·0883 (6)	0·9756 (4)		1·10	100·	
12	Si(10)	0·0582 (11)	−0·0054 (12)	0·1295 (8)	0·90 (8)	0·11 (6)	0·	
	Mn(10′)	0·0561 (6)	0·0025 (6)	0·6294 (4)		1·06	100·	
12	Si(14)	0·3050 (10)	0·0273 (15)	0·2538 (7)	0·60 (7)	−0·05 (6)	0·	
	Mn(14′)	0·3079 (6)	0·0275 (8)	0·7573 (4)		1·15	100·	
12	Mn(15)	0·2466 (4)	0·0210 (6)	0·3820 (4)	0·65 (7)	1·05 (6)	100·	
	MS(15′)	0·2386 (7)	0·0148 (10)	0·8821 (6)		0·22	27·	0·83
12	Mn(18)	0	0·0035 (9)	0	0·90 (11)	1·01 (8)	100·	
	MS(18′)	0	−0·0043 (11)	½		0·55	56·	0·99
12	Si(20)	0·0840 (11)	0·3758 (13)	0·2787 (8)	0·52 (7)	−0·19 (5)	0·	
	Mn(20′)	0·0842 (6)	0·3782 (7)	0·7753 (4)		1·20	100·	
12	Mn(22)	0·5269 (6)	0·3116 (6)	0·1856 (4)	0·83 (8)	1·01 (6)	100·	
	MS(22′)	0·5260 (8)	0·3199 (9)	0·6867 (6)		0·33	34·	0·86
12	MS(23)	0·2334 (7)	0·2146 (8)	0·4396 (5)	0·45 (6)	0·44 (5)	53·	0·97
	Mn(23′)	0·2300 (5)	0·2113 (6)	0·9378 (4)		1·09	100·	
12	Mn(25)	0·0863 (5)	0·3155 (7)	0·4076 (4)	0·72 (7)	0·92 (6)	100·	
	Si(25′)	0·0813 (10)	0·3143 (12)	0·9018 (7)		−0·07	0·	

* For atoms for which only parameters for the unprimed subcell are given, positional parameters were not varied in the final cycles with all data (except for atom 17, which is on a twofold axis in the subcell). The *z* value given for each of these atoms is for the unprimed subcell; that for the primed subcell is greater by ½. For the remaining atoms positional parameters in both subcells were allowed to vary in the final cycles.

† In the final refinements with all reflections, all atoms in either subcell which are mixtures were put in with a form factor corresponding to 58 at. % Mn, 42 at. % Si, and the actual electron content of each position was then specified with the multiplicity variable *m*, relative to unity for 58% Mn.

Mn(Fe) in the positions j in the unprimed and primed subcells are given by $a_j + y_j$ and $a_j - y_j$ (Table 5).

The intensity data for the subcell and the supercell were then combined and six cycles of refinement in which the scale factor and the positional parameters of the 2×16 atoms mentioned above (and of atom 17 which in the supercell is no longer on a twofold axis) were varied led to the agreement indices given in the second half of Table 2. The variation of these positional parameters reduced the R values for the superstructure reflections by about 4%.*

It should be noted from the values of the positional parameters for the unprimed and primed subcells in Table 5 that the shifts from the average structure resulting from positional refinements with all of the data are in many cases significant, judging from the estimated standard deviations as calculated in the usual manner, and that several of the shifts from the average positions are of the order of 0·05 Å. If these shifts are accepted as valid, many interatomic distances* must differ from those for the averaged subcell in Table 4 by that order or more. However, in view of the sparseness and weakness of the superstructure reflections and the fact that they do not provide the usual amount of overdetermination of the parameters refined with them, the significance of the shifts may be open to some question. This conclusion is strengthened by the fact that there is no discernible correlation, in magnitude or direction, of the major axes of the apparent vibrational ellipsoids with the shifts of subcell atoms from their average positions.

* A table of structure factors, based on the coordinates given in Table 5, and a list of interatomic distances, after refinement with all the data, have been deposited with the British Library Lending Division as Supplementary Publication No. SUP 32097 (25 pp.). Copies may be obtained through The Executive Secretary, International Union of Crystallography, 13 White Friars, Chester CH1 1NZ, England.

Description of the structure

The 'nets' perpendicular to y

Fig. 2 is a stereo picture of part of the average structure viewed down the y axis with the atoms at approxi-

* See previous footnote.

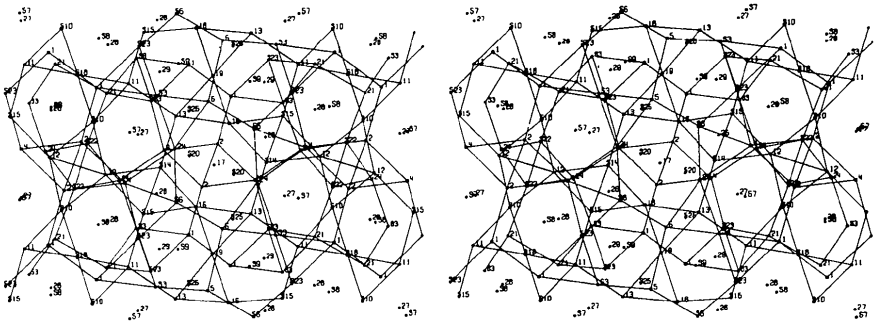

Fig. 2. Stereoscopic view produced by *ORTEP* (Johnson, 1965) of part of the substructure of the K phase in the direction of the $-b$ axis. For this and the other stereoscopic figures, atoms with CN > 12 are identified by their numbers, atoms with CN = 12 by their numbers preceded by S. Atom S 18 in the upper left is approximately at the origin, **a** is horizontal on the page, **c** is vertical. The layers at $y \sim -\frac{1}{4}$, 0, and $\frac{1}{4}$ are shown.

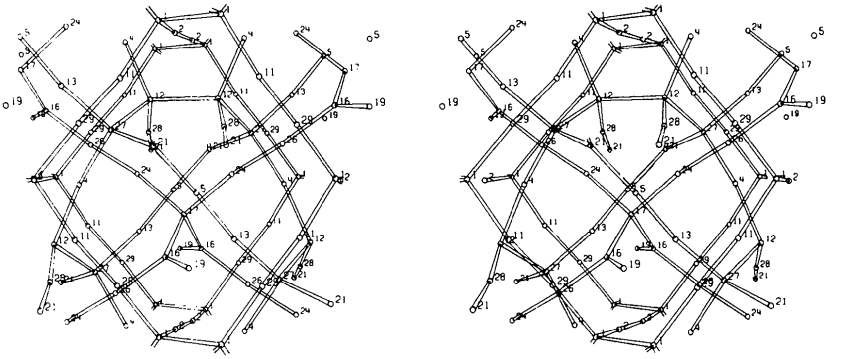

Fig. 3. Stereoscopic view produced by *ORTEP* of parts of the three interpenetrating 'major networks' of 6-coordinated bonds (*i.e.* bonds to ligands of SCN six) in the K phase in the direction of the $-c$ axis. Atom 17 in the upper left is at approximately 0, $\frac{1}{2}$, $\frac{1}{2}$; **a** is horizontal, **b** is vertical.

mately $y \sim -\frac{1}{4}$, 0, and $+\frac{1}{4}$ connected with line segments somewhat arbitrarily to form rumpled nets. Although the layers are far from planar they are presented this way largely because a ball-and-stick model of the structure which we have exhibited at meetings was constructed on the basis of them, and connecting atoms in this way makes some features of the structure easier to see. The atoms are designated by their numbers as previously assigned, the numbers of the CN 12 atoms being preceded by the letter S. The atoms chosen to form the layers at $y \sim \frac{1}{4}$ and $y \sim 0$ are connected to form pentagons and triangles, but in each layer around the twofold axis at the center of the unit cell there is a rumpled hexagon. The C centering is not apparent in the figure because the atoms chosen to form the layer at $y \sim -\frac{1}{4}$ have been connected into a pleated sheet of pentagons and triangles. It may be pointed out that if the K phase consisted of *planar* layers of this type, it would be the pentagonal analog of the σ phase (pentagons replacing hexagons: Shoemaker & Shoemaker, 1969; Kripyakevich & Yarmolyuk, 1971).

Interatomic distances and major networks

The K phase is a third example of an 'ideally' tcp structure that does not consist of *planar* layers stacked on top of each other. The other examples are the R phase (Komura, Sly & Shoemaker, 1960) and the δ phase (Shoemaker & Shoemaker, 1963). Only the 'regular' CN's of 12, 14, 15, and 16 occur, and all

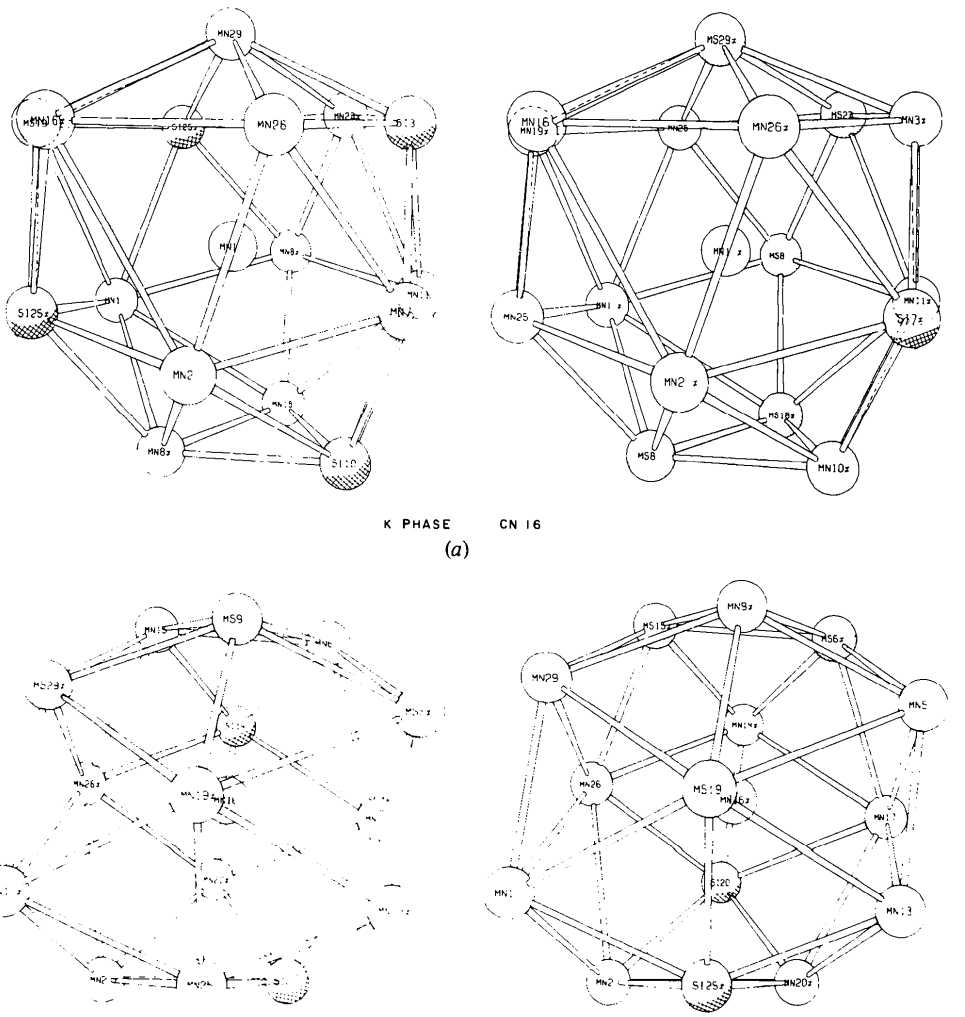

Fig. 4. Some CN polyhedra for atoms related by elements of pseudosymmetry in the superstructure of the K phase. (The prime is shown as $\neq$.) Si atoms are identified by cross-hatching, mixtures of Mn(Fe) and Si by stippling. (*a*) CN 16 polyhedra of Mn 1 (left) and Mn 1 $\neq$ (right). (*b*) CN 15 polyhedra of Mn 16 (left) and Mn 16 $\neq$ (right).

ligands have polyhedron surface coordination numbers (SCN) limited to five and six. In this the *K* phase differs from the *D* phase (Shoemaker & Shoemaker, 1976) in which all interstices are tetrahedral, but in which irregular CN's of 11 and 13 occur as well as some four-coordinated bonds (*i.e.* bonds to ligands with SCN four). The interatomic distances in the average structure are given in Table 4. The range they cover is from 2·324 to 3·297 Å, which is comparable with that in the *D* phase, Mn_5Si_2 (2·319–3·364 Å) and that in the ν phase, $Mn_{82}Si_{18}$ (2·211–3·279 Å). The 'major bonds' (those to ligands with SCN's of six) are marked in Table 4 by asterisks. They form three interlocking, non-interconnected networks, shown in Fig. 3, and describe the way the polyhedra for CN > 12 stack and interpenetrate each other. The network formed by atoms 17 (CN 16), 24 (CN 14), 26 (CN 14), 16 (CN 15), and 19 (CN 14) is very similar to the networks occurring in the δ phase. That going through atom 27 has two branches connecting CN 16 (27), CN 14 (13), CN 14 (5), and CN 15 (21) atoms as in the δ phase, but the other two branches consist of CN 16 atoms (12 and 27) and CN 14 atoms (4 and 28). The network formed by atoms 1 (CN 16), 11 (CN 14), 29 (CN 14) and 2 (CN 14) outlines the primitive unit cell of the *K* phase (and the δ phase). If atoms 1 were CN 15 rather than CN 16 a planar network as found in the σ phase would be formed.

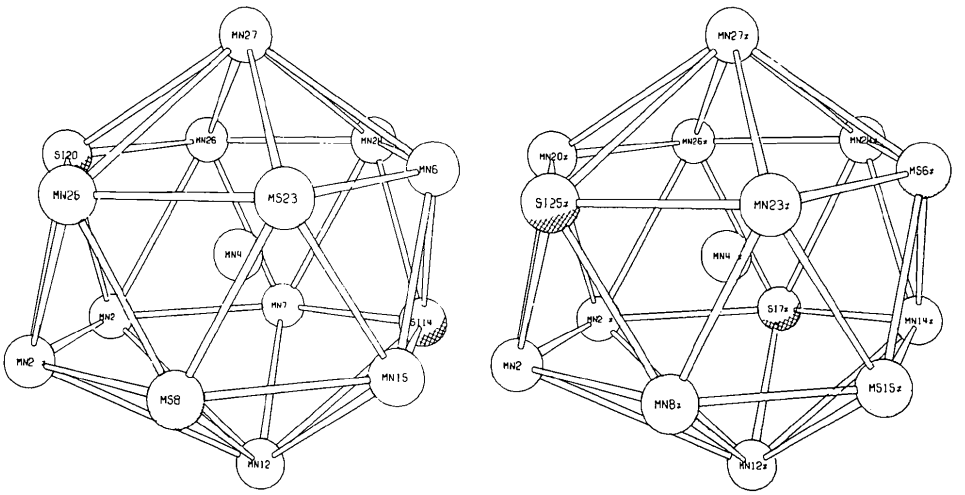

(*c*)

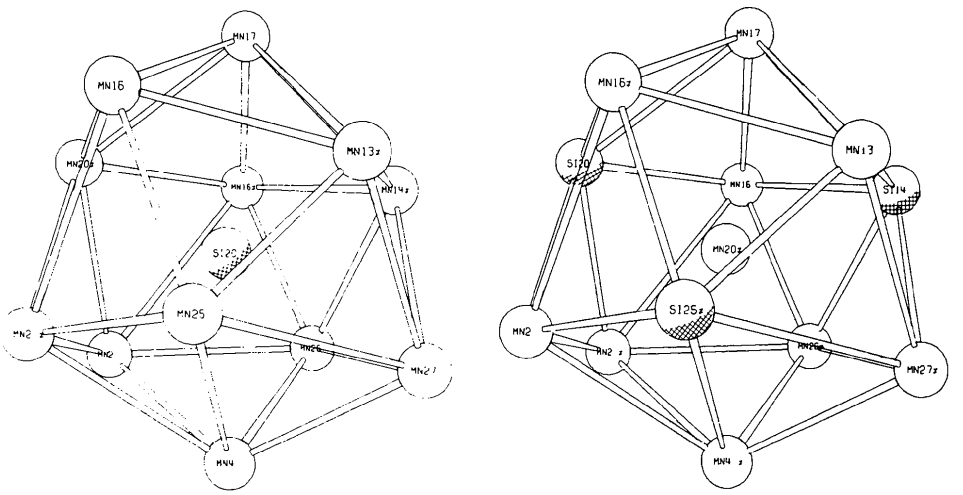

(*d*)

Fig. 4 (*cont.*). (*c*) CN 14 polyhedra of Mn 4 (left) and Mn 4 ≠ (right). (*d*) CN 12 polyhedra (icosahedra) of Si 20 (left) and Mn 20 ≠ (right).

The superstructure

As mentioned above, the superstructure results from an ordering of the atoms on the CN 12 sites which, in the average structure, were occupied by mixtures of Mn and Si atoms. Sites 3, 7, 10, 14, 20, 25 are occupied by Mn in one subcell while the corresponding sites in the other subcell are occupied by Si (see Fig. 1). Sites 6, 8, 9, 15, 18, 22, 23 which contain more than 50% Mn in the average structure are Mn in one subcell, while they are still mixtures in the other subcell. The same probably applies to the three CN 14 sites that may contain some Si in the average structure (5, 19, 29). All Si atoms in the superstructure are surrounded only by Mn(Fe) atoms. [The one possible exception is Si(25') (CN 12) which has as one of its neighbors 'MS(19)' (CN 14) which may have a small percentage of silicon.] Mn(Fe) atoms are surrounded by sites occupied by Si, Mn(Fe) or mixtures, and sites occupied by mixtures are surrounded by sites occupied by Mn(Fe) or mixtures. The average percentage Mn(Fe) in the first coordination shell increases with the decrease of the percentage Mn(Fe) of the central site, as was previously found for the ν phase, $Mn_{81.5}Si_{18.5}$ (Shoemaker & Shoemaker, 1971*a*) and the *X* phase, $Mn_{45}Co_{40}Si_{15}$ (Manor, Shoemaker & Shoemaker, 1972). Fig. 4 shows some of the CN polyhedra in the two halves of the superstructure cell, illustrating the difference in the environment of corresponding sites in the two subcells.

Relations to other tcp structures and near tcp structures

Table 6 lists some of the characteristics of tcp structures containing Mn and Si. The δ phase is included because of its structural relation with the *R* phase and the *K* phase. Only the ν or *N* phase has a plane-layered structure; all other structures listed contain rumpled layers. Three structures (α-Mn, δ phase and *D* phase) have rumpled σ-phase-type layers and their unit cells may be derived from the σ-phase unit cell by doubling of the *c* axis. This is also true for the primitive unit cell of the *K* phase. All structures, except α-Mn and the *D* phase, contain only the regular CN polyhedra of 12, 14, 15, and 16, and are thus ideally tcp. α-Mn contains polyhedra of CN 13 and has some non-tetrahedral interstices; the *D* phase contains polyhedra of CN 11 and 13, and has some four-coordinated bonds, but all interstices are tetrahedral.

In both non-planar tcp structures of the *R* phase and the δ phase directions can be found in which almost planar arrangements occur in triangles, five-membered, and six-membered rings. In the *R* phase straight rows of alternating pentagons and hexagons are closely confined to planes with hexagonal indices $(\bar{1}\bar{3}5)$ (Komura *et al.*, 1960, Fig. 4). In the *K* phase in the layers at $y \sim 0$ and $y \sim \frac{1}{4}$ shown in Fig. 2 there also occur straight rows (making an angle of about 20° with the horizontal) of pentagons, interrupted in the center by a hexagon. As pointed out these layers are, however, far from planar.

In the δ phase the $(04\bar{1})$ and $(40\bar{1})$ planes contain zigzag rows of hexagons alternating with zigzag rows of pentagons (Shoemaker & Shoemaker, 1963, Fig. 2). The corresponding plane in the *K* phase has (subcell) indices (441). Fig. 5 is a stereo view in the direction perpendicular to this plane showing all atoms within 1·30 Å perpendicular distance from the $(44\bar{1})$ plane passing through $\frac{1}{4}$, 0, 0, and from the parallel plane 2·12 Å normal distance below it. The horizontal direction on the page is along [110] and the vertical direction is along $[01\bar{4}]$. All atoms within 0·60 Å from the planes are connected by lines representing bonds. Although there are regions where the regularity is disturbed, one can clearly recognize zigzag rows of alternating pentagons and hexagons in a vertical direction, very similar to those occurring in the δ phase.

Although the ν phase and the *K* phase have compositions that are very similar, their structures seem to be entirely different. On comparing, however, the arrangements of the atoms in the (001) planes of the ν phase (Shoemaker & Shoemaker, 1971*a*, Fig. 3) and the $(20\bar{4})$ planes of the *K* phase, one finds some similarity. Fig. 6 is a stereo view in a direction perpendicular to $(20\bar{4})$. The $[20\bar{1}]$ direction is horizontal and the *y* axis is vertical. All atoms are shown within 1·30 Å normal distance from the $(20\bar{4})$ plane passing through 1, 0, $\frac{3}{4}$, and from the parallel plane below it at a normal distance of 2·10 Å. All atoms within 0·60 Å perpendicular distance from the two planes have been connected by lines representing bonds. The 'tiles' of six-membered rings in the ν phase are replaced in the *K* phase by a non-planar central six-membered ring (between atoms 2)

Table 6. *Crystal data for tcp structures in the* Mn—(Fe)—Si *system and for the* δ *phase*

Phase		Space group	*a* (Å)	*b* (Å)	*c* (Å)	β(°)	*Z*	Percentage sites with CN					
								11	12	13	14	15	16
*A*12	α-Mn	$I\bar{4}3m$	8·912				58		41	41			17
R	$Mn_{86}Si_{14}$	$R\bar{3}$	8·959			74·70	53		51		23	11	15
δ	$Mo_{50}Ni_{50}$	$P2_12_12_1$	9·108	9·108	8·852		56		43		36	14	7
K	$Mn_{77}Fe_4Si_{19}$	*C*2	13·362	11·645	8·734	90·53	110 × 2		45		35	7	13
ν or *N*	$Mn_{82}Si_{18}$	*Immm*	16·992	28·634	4·656		186		40		43	11	6
D	$Mn_{71}Si_{29}$	$P4_12_12$	8·910		8·715		56	14	29	14	14		29

surrounded by five-membered rings. A similar non-planar arrangement of five- and six-membered rings is found surrounding atom 18.

We wish to thank Professor Paul A. Beck of the University of Illinois for providing the *K*-phase samples. We are grateful to Drs M. Taylor, J. G. Keil, and P. C. Manor for experimental assistance while they were graduate students at Massachusetts Institute of Technology, and to Dr T. E. Hopkins of Oregon State University for assistance with the experimental and computational work. We thank Dr A. Zalkin of the Lawrence Berkeley Laboratory for making available to us his system of programs on the CDC 7600 computer. We thank Dr James Grow who, when a graduate student in this department, helped us to use the remote Corvallis terminal, kindly made available to us by the Environmental Protection Agency, Northwest Laboratory. We are happy to acknowledge the financial support of the Army Research Office (Durham) and the National Science Foundation.

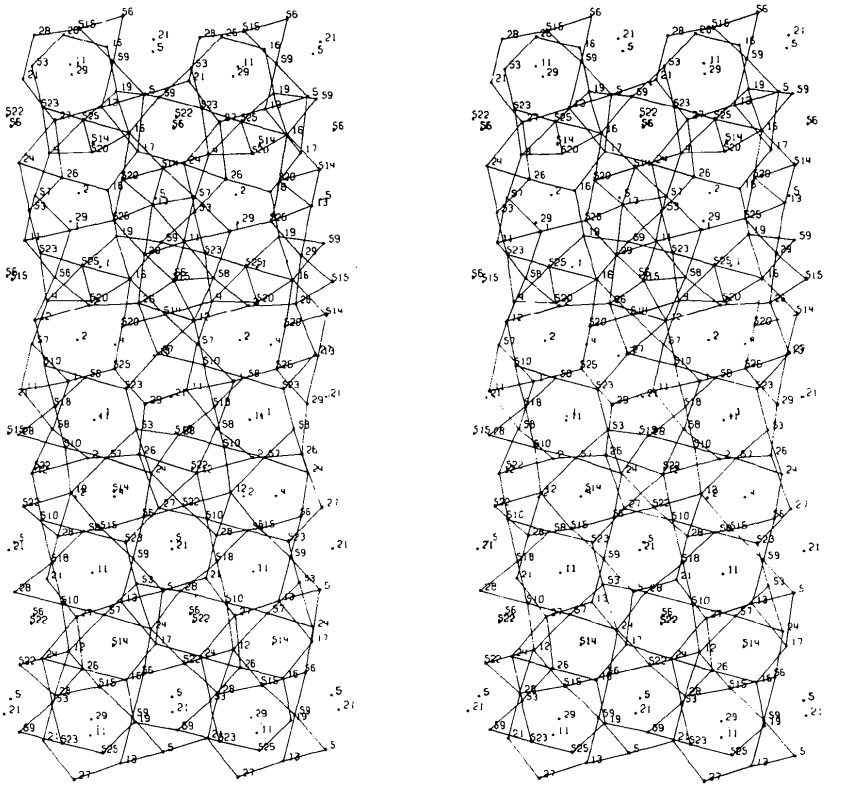

Fig. 5. *K* phase: stereo view of atoms within 1·30 Å normal distance from two net-planes parallel to (44$\bar{1}$) (subcell indices). Atoms within 0·60 Å from the two planes are connected by lines representing bonds. [110] is horizontal, [01$\bar{4}$] is vertical on the page.

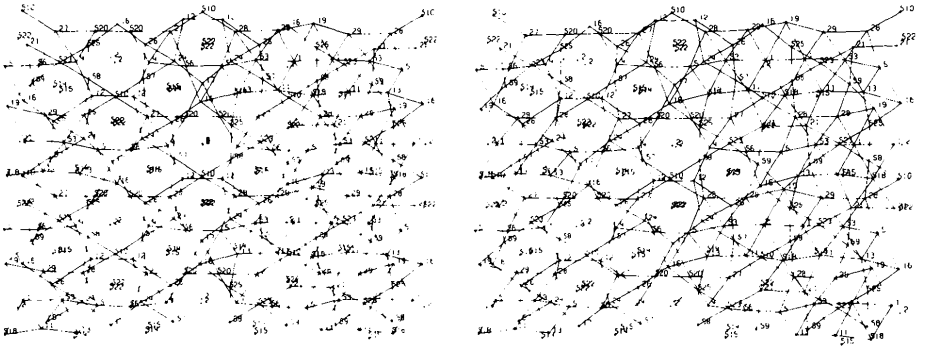

Fig. 6. *K* phase: stereo view of atoms within 1·30 Å normal distance from two net-planes parallel to (20$\bar{4}$) (subcell indices). Atoms within 0·60 Å from the two planes are connected by lines, representing bonds. [20$\bar{1}$] is horizontal, the *y* axis is vertical on the page.

References

BERGMAN, G. & SHOEMAKER, D. P. (1954). *Acta Cryst.* **7**, 857–865.

CROMER, D. T. & LIBERMAN, D. (1970). *J. Chem. Phys.* **53**, 1891–1898.

FRANK, F. C. & KASPER, J. S. (1959). *Acta Cryst.* **12**, 483–499.

GUPTA, K. P. (1964). *Trans. AIME*, **230**, 253–254.

International Tables for X-ray Crystallography (1962). Vol. III. Birmingham: Kynoch Press.

JOHNSON, C. K. (1965). *ORTEP*. Oak Ridge National Laboratory Report ORNL-3794.

KOMURA, Y., SLY, W. G. & SHOEMAKER, D. P. (1960). *Acta Cryst.* **13**, 575–585.

KRIPYAKEVICH, P. I. & YARMOLYUK, YA. P. (1971). *Dopov. Akad. Nauk. Ukr. RSR*, A**33**, 460–463.

MANOR, P. C., SHOEMAKER, C. B. & SHOEMAKER, D. P. (1972). *Acta Cryst.* B**28**, 1211–1218.

SHOEMAKER, C. B. & SHOEMAKER, D. P. (1963). *Acta Cryst.* **16**, 997–1009.

SHOEMAKER, C. B. & SHOEMAKER, D. P. (1969). *Developments in the Structural Chemistry of Alloy Phases*, edited by B. C. GIESSEN, pp. 107–139. New York: Plenum.

SHOEMAKER, C. B. & SHOEMAKER, D. P. (1971*a*). *Acta Cryst.* B**27**, 227–235.

SHOEMAKER, C. B. & SHOEMAKER, D. P. (1971*b*). *Mh. Chem.* **102**, 1643–1666.

SHOEMAKER, C. B. & SHOEMAKER, D. P. (1976). *Acta Cryst.* B**32**, 2306–2313.

ZACHARIASEN, W. H. (1963). *Acta Cryst.* **16**, 1139–1144.

Acta Cryst. (1977). B**33**, 754–762

Structural Chemistry of Layered Cyclophanes. I. Molecular Structure of a Triple-Layered [2.2]Metacyclophane (*ud* Isomer) and of a [2.2]Metacyclophane Redetermined at −160°C

BY YASUSHI KAI, NORITAKE YASUOKA AND NOBUTAMI KASAI

Department of Applied Chemistry, Faculty of Engineering, Osaka University, Yamadakami, Suita, Osaka 565, *Japan*

(*Received* 5 *July* 1976; *accepted* 10 *August* 1976)

The molecular structure of one of the two geometrical isomers of triple-layered [2.2]metacyclophane was determined from three-dimensional X-ray data collected on a four-circle diffractometer. The *ud* isomer crystallizes in the monoclinic space group $P2_1/c$ with four molecules per unit cell; a = 11·659 (1), b = 11·715 (1), c = 14·678 (1) Å and β = 107·69 (1)°. The structure was solved by the direct method and refined by block-diagonal least squares to an R of 0·048 for 2569 observed reflexions. The mean length of the methylene bridges is 1·565 Å. The bond distance between the bridging C and central benzene is 1·515 Å, which is significantly longer than that between the bridging C and terminal benzene, 1·506 Å. The molecular structure of [2.2]metacyclophane was redetermined from the X-ray data at −160°C to obtain standard data of high accuracy for the cyclophane compounds. The final R value was 0·050 for 2287 observed reflexions and the e.s.d.'s were σ(C–C) = 0·001 Å, σ(C–C–C) = 0·1°. The bond distance between the bridging C atoms is 1·568 Å. A comparison of these compounds shows an interesting addition effect of the two terminal benzene rings on the out-of-plane deformation of the central benzene ring.

Introduction

Layered cyclophanes are compounds which are expected to have highly strained molecular structures and specific physical properties. The structural chemistry of double-layered cyclophanes has been actively studied so far, but only a few structural studies have been reported for the multilayered cyclophanes. As the multilayered cyclophanes are supposed to have more constrained structures than those of double-layered cyclophanes, the determination of their molecular structures will reveal more remarkable physical properties than those found in their constituent double-layered cyclophanes.

Triple-layered [2.2]metacyclophanes have been synthesized by Umemoto, Otsubo & Misumi (1974). Two geometrical isomers were postulated from the nuclear Overhauser effect in PMR spectra. To distinguish these isomers, the symbols *ud* (u = up, d = down) and *uu* were given to the zigzag and stair-like isomers respectively. Easy thermal isomerization of the *uu* isomer to *ud* was observed by PMR investigations in toluene-d_8